Theoretical Investigation of the Selective C═C Hydrogenation of Unsaturated Aldehydes Catalyzed by [{$RuCl_2$(*m*tppms)$_2$}$_2$] in Acidic Media

Gábor Kovács,[†,‡] Gregori Ujaque,[§] Agustí Lledós,*[,§] and Ferenc Joó*[,†,‡]

Institute of Physical Chemistry, University of Debrecen, Debrecen 10, H-4010 Hungary, Research Group of Homogeneous Catalysis, Hungarian Academy of Sciences, Debrecen 10, P.O. Box 7, H-4010 Hungary, and Departament de Química, Universitat Autònoma de Barcelona, 08193 Bellaterra (Barcelona), Spain

Received October 28, 2005

Density functional theory has been applied to identify possible reaction intermediates for the catalytic C═C hydrogenation of cinnamaldehyde, which occurs in acidic aqueous solutions in the presence of water-soluble ruthenium phosphine complexes. On the basis of ONIOM calculations, two different active species and, hence, two pathways were proposed. The C═C bond hydrogenation takes place through the insertion of the terminal carbon atom into the Ru−H bond and subsequent protonation of the other carbon by hydroxonium ions present in the solution. We find that water is directly involved in several steps of the reaction, either as a protonating/deprotonating agent or as a coordinating ligand. Selectivity against C═O hydrogenation is due to the much higher barrier of either C insertion or O insertion into the Ru−H bond as compared to that of the C insertion in the case of the C═C functionality.

Introduction

Hydrogenation reactions proceeding in aqueous solutions catalyzed by organometallic complexes present an area of homogeneous catalysis of great importance.[1−2] Aqueous phase catalysis not only provides special reaction conditions concerning the distinct properties of water as contrasted with those of nonpolar organic solvents but also offers the possibility for avoiding the problem of catalyst separation by the application of two-phase (aqueous−organic) systems.[3−4] In addition, water is often cited as an ideal solvent, since it is cheap, readily available, nontoxic, and totally compatible with the environment.[5−6]

One of the most important characteristics of aqueous systems is that water does not behave as a mere solvent but can play an active role in the reactions.[7−10] The pH of the solution can alter the presence of the different catalytically active hydride species,[11−12] whereas water molecules can coordinate to the metal centers, as observed on many occasions, can take part in proton-transfer reactions, and can form hydrogen bonds with different parts of the complex catalysts.[13−17] These effects give rise to different mechanistic possibilities for reactions compared to the possibilities in organic solvents.

One of the most interesting hydrogenation reactions is the selective reduction of α,β-unsaturated aldehydes.[18−19] In aqueous solution, the ruthenium(II) complex of *m*tppms ((*m*-sulfonatophenyl)diphenylphosphine) was tested thoroughly by Joó and co-workers, for the hydrogenation of cinnamaldehyde (3-phenylpropenal).[11,20] The reactions were run at elevated temperatures (80 °C) and atmospheric hydrogen pressure, and selective reduction of the different double bonds was obtained, depending on the pH of the reaction medium. In acidic solutions the product of the reaction was exclusively dihydrocinnamaldehyde, formed by the saturation of the olefinic double bond, while in basic solution selective hydrogenation of the C═O bond took place to yield cinnamyl alcohol. These observations were explained by the distribution of the catalytically active hydride species that are present in the solution as a function of the pH. On the basis of potentiometric and NMR results (^{1}H and ^{31}P),

* To whom correspondence should be addressed. E-mail: agusti@klingon.uab.es (A.L.); jooferenc@delfin.unideb.hu (F.J.).
† University of Debrecen.
‡ Hungarian Academy of Sciences.
§ Universitat Autònoma de Barcelona.

(1) Peruzzini, M., Poli, R., Eds. *Recent Advances in Hydride Chemistry*; Elsevier: Amsterdam, 2003.
(2) Kritsjánsdottír, S. S.; Norton, J. R. Acidity of Hydrido Transition Metal Complexes in Solution. In *Transition Metal Hydrides*; Dedieu, A., Ed.; VCH: Weinheim, Germany, 1992.
(3) Joó, F. *Aqueous Organometallic Catalysis*; Kluwer: Dordrecht, The Netherlands, 2001.
(4) Adams, D. J.; Dyson, P. J.; Tavener, S. J. *Chemistry in Alternative Reaction Media*; Wiley: Chichester, U.K., 2004.
(5) Joó, F.; Kathó, Á. In *Aqueous Phase Organometallic Catalysis*, 2nd ed.; Cornils, B., Herrmann, W. A., Eds.; Wiley-VCH: Weinheim, Germany, 2004.
(6) Cornils, B., Herrmann, W. A., Horváth, I. T., Leitner, W., Mecking, S., Olivier-Bourbignon, H., Vogt, D., Eds. *Multiphase Homogeneous Catalysis*; Wiley-VCH: Weinheim, Germany, 2005.
(7) Joó, F. In *Encyclopedia of Catalysis*; Horváth, I. T., Ed.; Wiley: New York, 2002; Vol. I.
(8) Laghmari, M.; Sinou, D. *J. Mol. Catal.* **1991**, *66*, L15.
(9) Joó, F.; Csiba, P.; Bényei, A. C. *J. Chem. Soc., Chem. Commun.* **1993**, 1602.
(10) Joó, F.; Nádasdi, L.; Bényei, A. C.; Darensbourg, D. J. *J. Organomet. Chem.* **1996**, *512*, 45.
(11) Joó, F.; Kovács, J.; Bényei, A. C.; Kathó, Á. *Angew. Chem.* **1998**, *110*, 1024; *Angew. Chem., Int. Ed.* **1998**, *37*, 969.
(12) Joó, F.; Kovács, J.; Bényei, A. C.; Nádasdi, L.; Laurenczy, G. *Chem. Eur. J.* **2001**, *7*, 241.
(13) Belkova, N.; Besora, M.; Epstein, L. M.; Lledós, A.; Maseras, F.; Shubina, E. S. *J. Am. Chem. Soc.* **2003**, *125*, 7715.
(14) Orlova, G.; Scheiner, S.; Kar, T. *J. Phys. Chem. A* **1999**, *103*, 514.
(15) Chu, H. S.; Xu, Z.; Ng, S. M.; Lau, C. P.; Lin, Z. *Eur. J. Inorg. Chem.* **2000**, 993.
(16) Kovács, G.; Schubert, G.; Joó, F.; Pápai, I. Submitted for publication in *Catal. Today*.
(17) Kovács, G.; Schubert, G.; Joó, F.; Pápai, I. *Organometallics* **2005**, *24*, 3059.
(18) Grosselin, J. M.; Mercier, C.; Allmang, G.; Grass, F. *Organometallics* **1991**, *10*, 2126.
(19) Hernandez, M.; Kalck, P. *J. Mol. Catal.* **1997**, *117*, 131.
(20) Joó, F.; Kovács, J.; Bényei, A. C.; Kathó, Á. *Catal. Today* **1998**, *42*, 441.

10.1021/om050929y CCC: $33.50
Publication on Web 01/19/2006

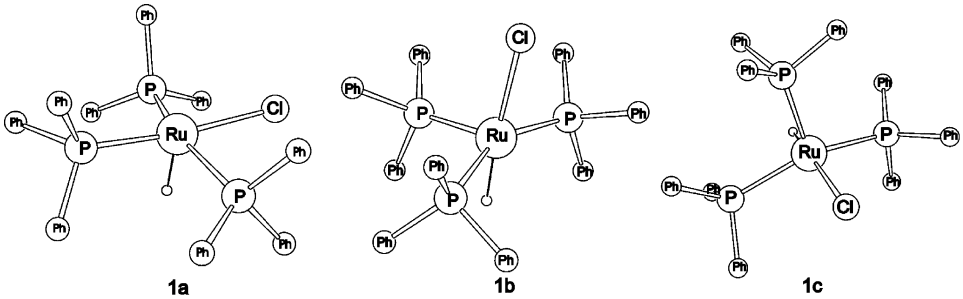

Figure 1. Optimized structures for the different isomers of $[RuHCl(PPh_3)_3]$.

under ambient pressure in acidic media $[RuHCl(m\text{tppms})_3]$ was detected as the major species, whereas under neutral and basic conditions the dominant ruthenium species was $[RuH_2(m\text{tppms})_4]$.[11,20] Thus, $[RuHCl(m\text{tppms})_3]$ was thought to be active in the catalysis of the C═C double bond and inactive in the reduction of the C═O functionality, while $[RuH_2(m\text{tppms})_4]$ was considered to have the opposite selectivity.

Despite the detection of the major species, the mechanistic features of the reaction have remained unknown. In addition, the origin of the selectivity in the hydrogenation has not been explained yet. The present work is devoted to studying the selective reduction of C═C over C═O under *acidic* conditions, whereas the study of the reaction mechanism in *basic* solutions will be described in another work. The experimental results were used as starting points, and theoretical methods were applied to study the reaction mechanism.

Computational Details

Calculations were performed using the Gaussian03 series of programs.[21] Geometry optimizations were done using the density functional theory (DFT) with the hybrid B3LYP functional.[22−24] Effective core potentials (ECP) and its associated double-ζ LANL2DZ basis set were used for ruthenium atoms.[25−27] The 6-31G* basis set was used for the rest of the atoms (H, C, O, P, and Cl).[28−29]

The complex $[RuHCl(PH_3)_3]$ was used as a model for the catalyst to analyze the reaction mechanism. We first performed an analysis on the different isomers of the complex with the bulky phosphines (PPh_3 ligands were used in the calculations) in order to obtain their structures and compute their relative stabilities. Hence, to perform this structural analysis the different isomers of the $[RuHCl(PPh_3)_3]$ complex (the structure of which is not considered to differ significantly from that of $[RuHCl(m\text{tppms})_3]$) were fully optimized using the ONIOM(B3LYP/UFF) method as implemented in Gaussian03.[30−31] The part of the molecule described at the high level was the same as for the model complex (with the same functional and basis set), whereas the rest of the system (the phenyl rings of the PPh_3 ligands) was described at the molecular mechanics level (UFF). The relative energies for these structures were obtained by single-point calculations at the DFT level on the ONIOM optimized structures. These calculations were performed with Jaguar[32] using the same functional (B3LYP) and the LACVP basis set for ruthenium[25] and the 6-31G* basis set for the other atoms.

For the transition states normal-coordinate analysis was performed to verify them, and for each transition structure intrinsic reaction coordinate (IRC) routes in both directions to the corresponding minima were calculated. If the IRC calculations failed to reach the minima, geometry optimizations from the initial phase of the IRC path were performed.

Results and Discussion

Hydrogenation of cinnamaldehyde catalyzed by $[\{RuCl_2(m\text{tppms})_2\}_2]$ in acidic solutions always resulted in the selective reduction of the olefin double bond and in the formation of dihydrocinnamaldehyde.[11,20] Under acidic conditions $[RuHCl(m\text{tppms})_3]$ was shown to be the major species, and in fact, this complex is thought to be active in the reduction of C═C functionalities. A detailed mechanistic picture could not be obtained from experimental results, since no reaction intermediates were detected by spectroscopic (NMR or IR) methods.

We applied theoretical methods (DFT) to investigate the reaction mechanism of this process. $[RuHCl(PH_3)_3]$ and acrolein (CH_2═CH−CHO) were used as a model system for the calculations. The reduction of acrolein to 1-propanal is shown in eq 1, and the total energy change calculated for the reaction is −36.5 kcal/mol.

$$CH_2{=}CHCHO + H_2 \rightarrow CH_3CH_2CHO \qquad (1)$$

Structure of the Active Species. Since the structure of the active species could not be inferred by experimental methods, the first step was the analysis of the possible isomers of the real system using PPh_3 as the phosphine ligand. The structure and the energy of the various isomers were calculated by means of the ONIOM (B3LYP/UFF) method. ONIOM (B3LYP/UFF) calculations with the PPh_3 ligands gave three relevant isomers, **1a**−**c** (Figure 1), with relative energies of 0.0, 1.4, and 14.5 kcal/mol, respectively. Nevertheless, isomer **1a** cannot be a reactive isomer in any type of reduction process, since the vacant

(21) Frisch, M. J.; Trucks, G. W.; Schlegel, H. B.; Scuseria, G. E.; Robb, M. A.; Cheeseman, J. R.; Montgomery, J. A., Jr.; Vreven, T.; Kudin, K. N.; Burant, J. C.; Millam, J. M.; Iyengar, S. S.; Tomasi, J.; Barone, V.; Mennucci, B.; Cossi, M.; Scalmani, G.; Rega, N.; Petersson, G. A.; Nakatsuji, H.; Hada, M.; Ehara, M.; Toyota, K.; Fukuda, R.; Hasegawa, J.; Ishida, M.; Nakajima, T.; Honda, Y.; Kitao, O.; Nakai, H.; Klene, M.; Li, X.; Knox, J. E.; Hratchian, H. P.; Cross, J. B.; Bakken, V.; Adamo, C.; Jaramillo, J.; Gomperts, R.; Stratmann, R. E.; Yazyev, O.; Austin, A. J.; Cammi, R.; Pomelli, C.; Ochterski, J. W.; Ayala, P. Y.; Morokuma, K.; Voth, G. A.; Salvador, P.; Dannenberg, J. J.; Zakrzewski, V. G.; Dapprich, S.; Daniels, A. D.; Strain, M. C.; Farkas, O.; Malick, D. K.; Rabuck, A. D.; Raghavachari, K.; Foresman, J. B.; Ortiz, J. V.; Cui, Q.; Baboul, A. G.; Clifford, S.; Cioslowski, J.; Stefanov, B. B.; Liu, G.; Liashenko, A.; Piskorz, P.; Komaromi, I.; Martin, R. L.; Fox, D. J.; Keith, T.; Al-Laham, M. A.; Peng, C. Y.; Nanayakkara, A.; Challacombe, M.; Gill, P. M. W.; Johnson, B.; Chen, W.; Wong, M. W.; Gonzalez, C.; Pople, J. A. *Gaussian 03*, revision C.02; Gaussian, Inc.: Wallingford, CT, 2004.

(22) Becke, A. D. *J. Chem. Phys.* **1993**, *98*, 5648.

(23) Lee, C.; Yang, W.; Parr, R. G. *Phys. Rev. B* **1988**, *37*, 785.

(24) Stephens, P. J.; Devlin, F. J.; Chabalowski, C. F.; Frisch, M. J. *J. Phys. Chem.* **1994**, *98*, 11623.

(25) Hay, P. J.; Wadt, W. R. *J. Chem. Phys.* **1985**, *82*, 270.

(26) Wadt, W. R.; Hay, P. J. *J. Chem. Phys.* **1985**, *82*, 284.

(27) Hay, P. J.; Wadt, W. R. *J. Chem. Phys.* **1985**, *82*, 299.

(28) Hariharan, P. C.; Pople, J. A. *Mol. Phys.* **1974**, *27*, 209.

(29) Rassolov, V. A.; Ratner, M. A.; Pople, J. A.; Redfern, P. C.; Curtiss, L. A. *J. Comput. Chem.* **2001**, *22*, 976.

(30) Dapprich, S.; Komáromi, I.; Byun, K. S.; Morokuma, K.; Frisch, M. J. *J. Mol. Struct. (THEOCHEM)* **1999**, *462*, 1.

(31) Vreven, T.; Morokuma, K.; Farkas, Ö; Schlegel, H. B.; Frisch, M. J. *J. Comput. Chem.* **2003**, *24*, 760.

(32) Jaguar 4.1; Schrödinger, Inc., Portland, OR, 1991−2000.

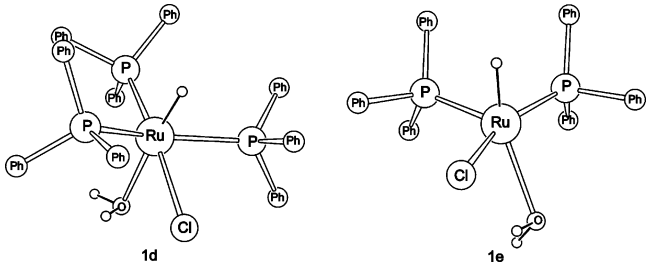

Figure 2. Optimized structures for $[RuHCl(H_2O)(PPh_3)_3]$ (**1d**) and $[RuHCl(H_2O)(PPh_3)_2]$ (**1e**).

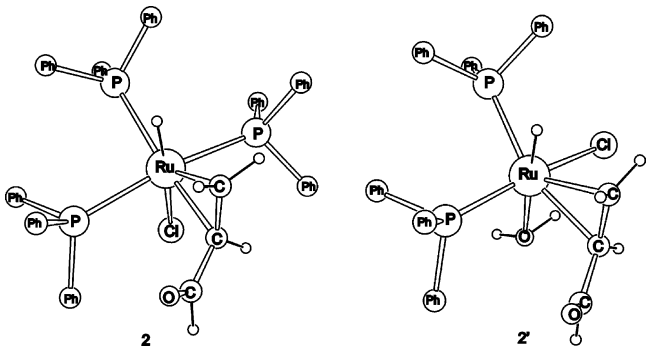

Figure 3. Optimized structures for $[RuHCl(C{=}C)(PPh_3)_3]$ (**2**) and $[RuHCl(H_2O)(C{=}C)(PPh_3)_2]$ (**2′**).

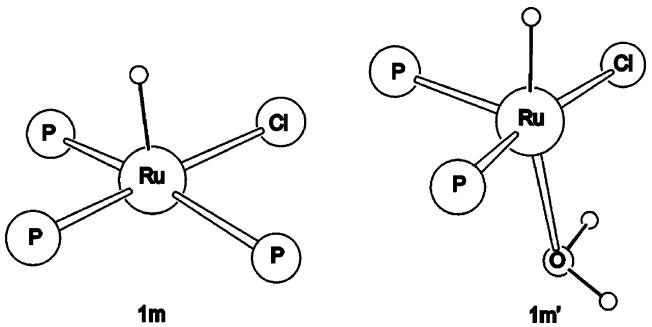

Figure 4. Optimized structures for $[RuHCl(PH_3)_3]$ (**1m**) and $[RuHCl(H_2O)(PH_3)_2]$ (**1m′**).

site for coordinating the substrate is in a position trans to the hydride ligand. Hence, **1a** is strongly unfavorable for any kind of hydride transfer, which is thought to be the first step of this reaction.

Table 1. Activation Barriers (kcal/mol) Calculated for the Carbon Insertion into the Ru−H Bond in Different Models of $[RuHCl(C{=}C)(PH_3)_3]$ Type Complexes

	2m (acrolein)	**2m*** (cinnamaldehyde)	**2a** (acrolein)	**2a*** (cinnamaldehyde)
$\Delta E^{\ddagger}$ (kcal/mol)	5.3	7.8	13.9	13.5

On the basis of experimental data, $[RuHCl(m\text{tppms})_3]$ was detected as the major species in these systems in acidic medium.[11] In addition, a decrease in the catalytic activity was found if the [Ru]:[*m*tppms] ratio was more than 1:2.[33] These observations drove us to consider two possible reaction routes in this process. One possible way consists of the rearrangement of **1a** to **1b**, where the vacant coordination site lies cis to the hydride ligand; isomer **1b** is only 1.4 kcal/mol higher in energy than isomer **1a**. Coordination of the olefin to this vacant site allows the formation of intermediate **2**; the associated energy for this process is only 2.0 kcal/mol.

The other reaction pathway includes the initial coordination of a water molecule to the vacant site and the subsequent elimination of a phosphine ligand. After these steps, the vacant site lies now cis to the hydride ligand, and the coordination of acrolein lets the initial hydrogenation step occur. Coordination of a water molecule leads to the formation of **1d** (Figure 2), which is an energetically favorable reaction by 10.0 kcal/mol. The coordination of water could facilitate the dissociation of one of the phosphine ligands to form **1e** (Figure 2), in a slightly endothermic reaction (+6.3 kcal/mol). At this point no further rearrangement is required for the coordination of the olefin in a position cis to the hydride. The process, which leads to the formation of intermediate **2′**, is favorable by 5.8 kcal/mol. Therefore, this is an alternative starting point for the reaction mechanism. This second path has a −9.5 kcal/mol energy balance, which is energetically more favorable than the 3.4 kcal/mol energy balance obtained for the first route. On the basis of these findings, both **2** and **2′** (Figure 3) can be starting points for the reaction.

The mechanistic calculations, however, and the reaction energy profile were done on a model system (substituting the

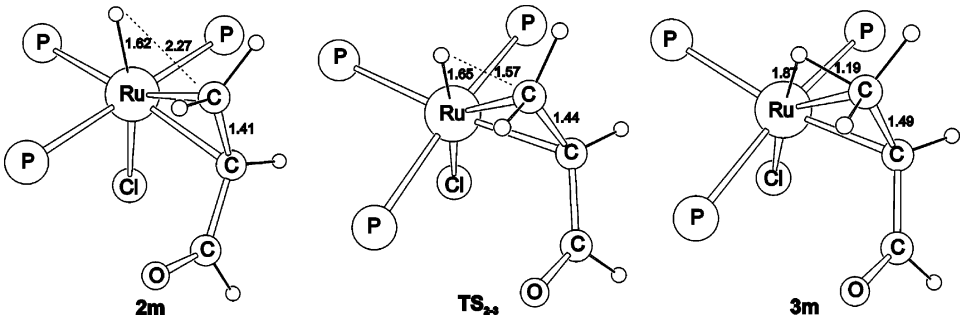

Figure 5. Optimized structures with selected bond lengths in structures representing the terminal carbon insertion in complex **2m**.

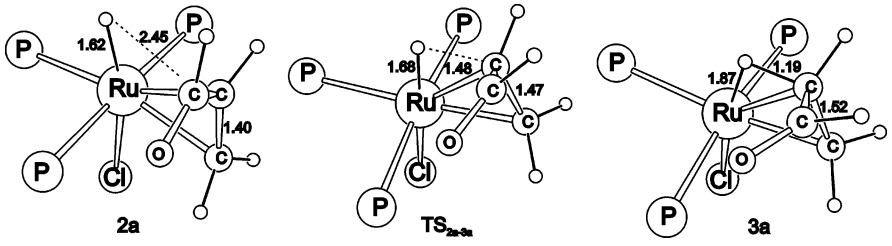

Figure 6. Optimized structures with selected bond lengths representing the carbon insertion in complex **2a**.

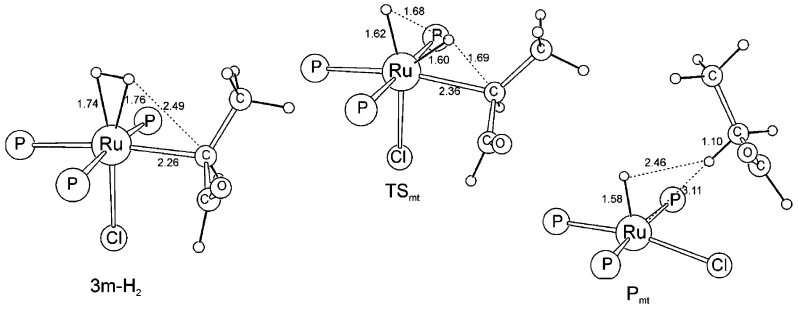

Figure 7. Optimized structures with selected bond lengths representing the σ-bond metathesis process between the coordinated η^2-H_2 and alkyl groups.

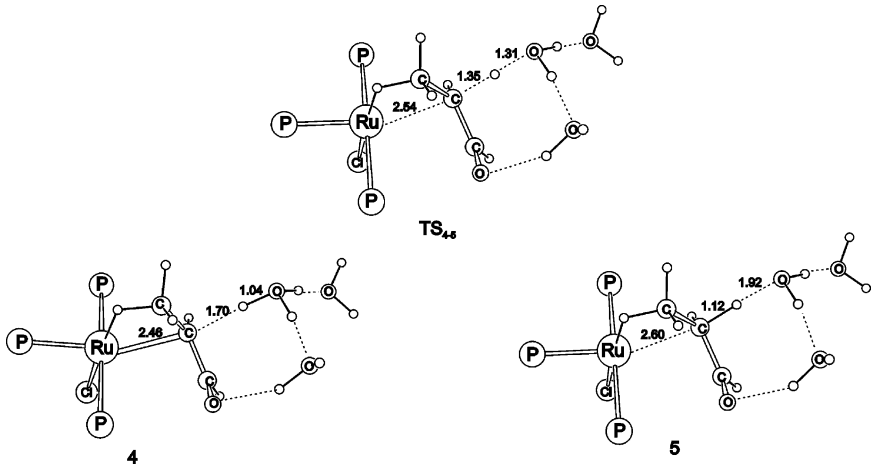

Figure 8. Optimized structures with selected bond lengths in structures representing the protonation of the carbon in complex **4**.

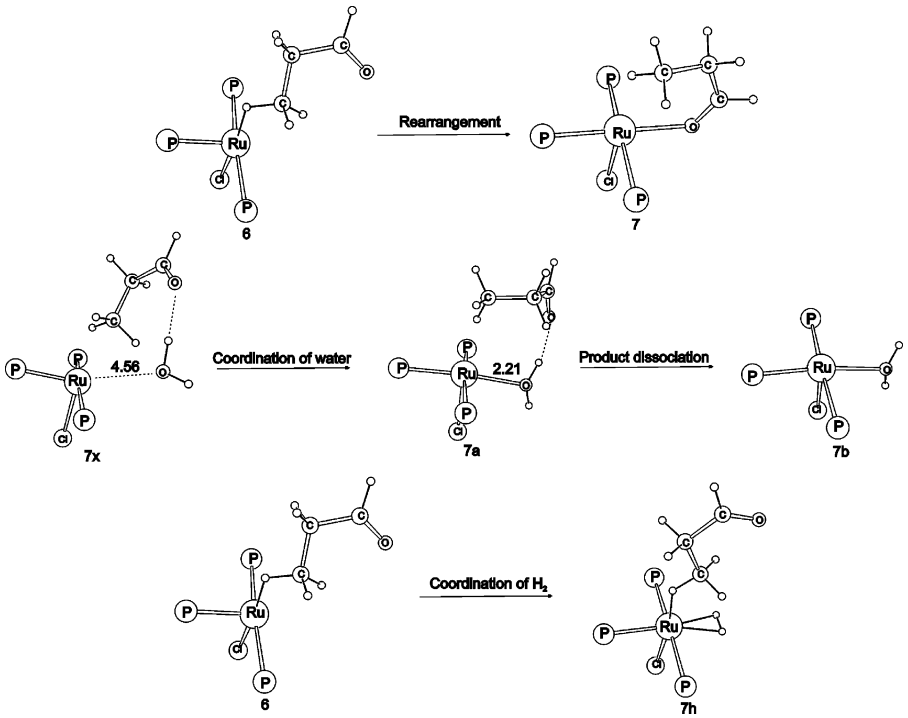

Figure 9. Optimized structures showing the possible further reactions of complex **6**.

real phosphines by PH_3) at the DFT/B3LYP level. In principle, steric effects should not be important in further reaction steps. The model starting compounds are **1m** for **1a** and **1m′** for **1e** (Figure 4.). With these two complexes as the starting points, two different pathways (paths I and II) have been explored.

Reaction Mechanism Starting from Complex 1m (Path I). The coordination of acrolein via its π(C═C) bond to the ruthenium center of **1m** leads to **2m**, which is the model compound for **2**, as shown in Figure 5. The energy change for the coordination is −13.4 kcal/mol. The first step of the reduction is terminal C insertion into the Ru−H bond, which takes place through the formation of $\mathbf{TS_{2-3}}$; this species lies

(33) Tóth, Z.; Joó, F.; Beck, M. T. *Inorg. Chim. Acta* **1980**, *42*, 153.

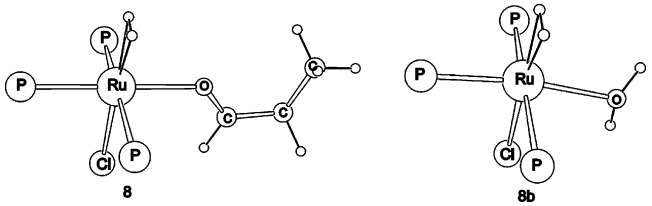

Figure 10. Optimized structures for complexes **8** and **8b**.

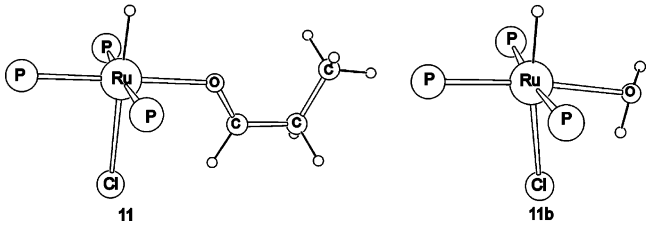

Figure 13. Optimized structures for complexes **11** and **11b**.

5.3 kcal/mol above complex **2m**. The product of this reaction is the agostic intermediate **3m**, in which the carbon−carbon bond is 1.5 Å. This is almost 0.1 Å longer than it was in complex **2m**, and the energy is 0.8 kcal/mol higher than that of **2m**. The C−H bond distance in complex **3m** is 1.19 Å, proving its agostic nature. The Ru−C (2.39 Å) and Ru−H distances (1.87 Å) also agree with the presence of a strong agostic interaction in **3m**. The structures representing this hydride transfer are shown in Figure 5.

In addition, another process was also examined, where the insertion is performed by the carbon atom adjacent to the carbonyl group instead of the terminal carbon atom. In this reaction path the corresponding stationary points are **2a**, $\mathbf{TS}_{\mathbf{2a-3a}}$, and **3a**. In **2a**, acrolein is also coordinated through its π(C=C) bond; however, the orientation of the substrate is different from that in **2m**. **2a** lies 0.4 kcal/mol above **2m**, and assuming a fast preequilibrium between the two complexes, the barriers for the hydride transfer are referenced to complex **2m**. The energy barrier in this case was 14.3 kcal/mol, which is much less favorable than the insertion of the terminal carbon atom. The structures representing this process are shown in Figure 6.

Additionally, calculations were also performed with the real substrate (cinnamaldehyde) to ensure that the hydride transfer in **2m** is more favorable than in **2a**, also in the case of the actual aldehyde. The barriers obtained with acrolein and cinnamaldehyde are shown in Table 1.

These energy values show that the transfer to the terminal carbon is much more favorable with either the model or the real substrate, indicating that the application of the model substrate does not cause significant changes in the energetics.

Although complex **3m** does not contain a coordination vacancy, approach of an H_2 molecule could lead to the rupture

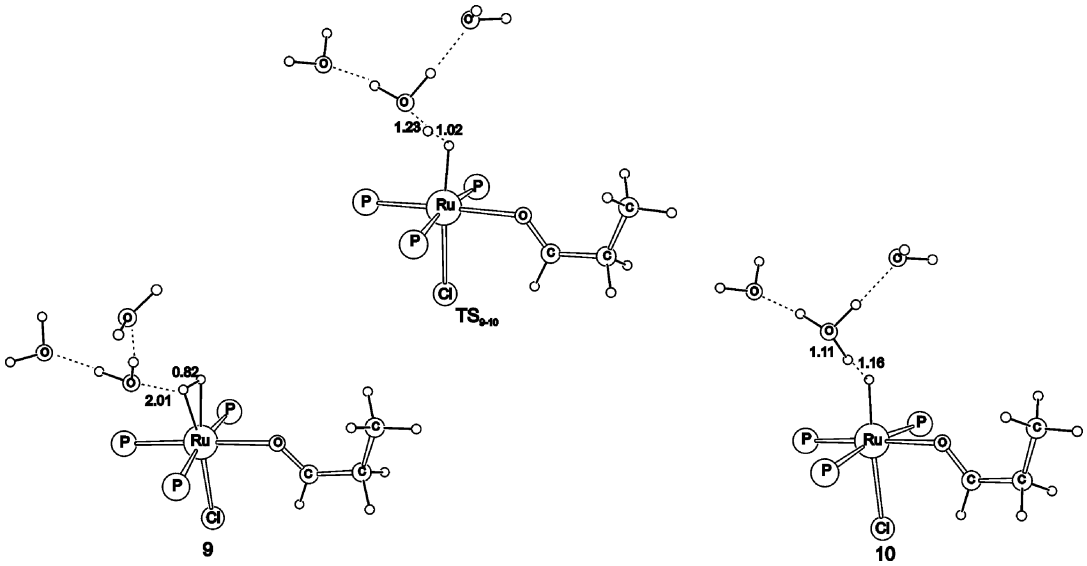

Figure 11. Optimized structures and selected bond lengths representing the deprotonation of complex **9**.

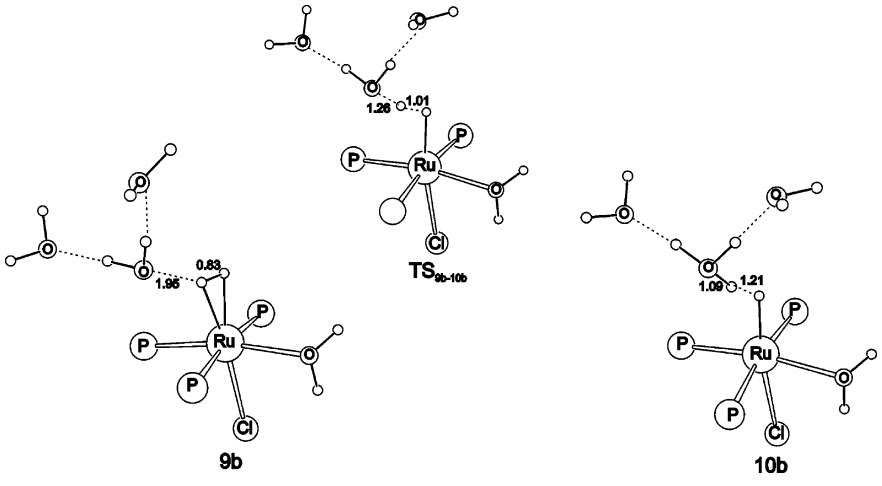

Figure 12. Optimized structures and selected bond lengths representing the deprotonation of complex **9b**.

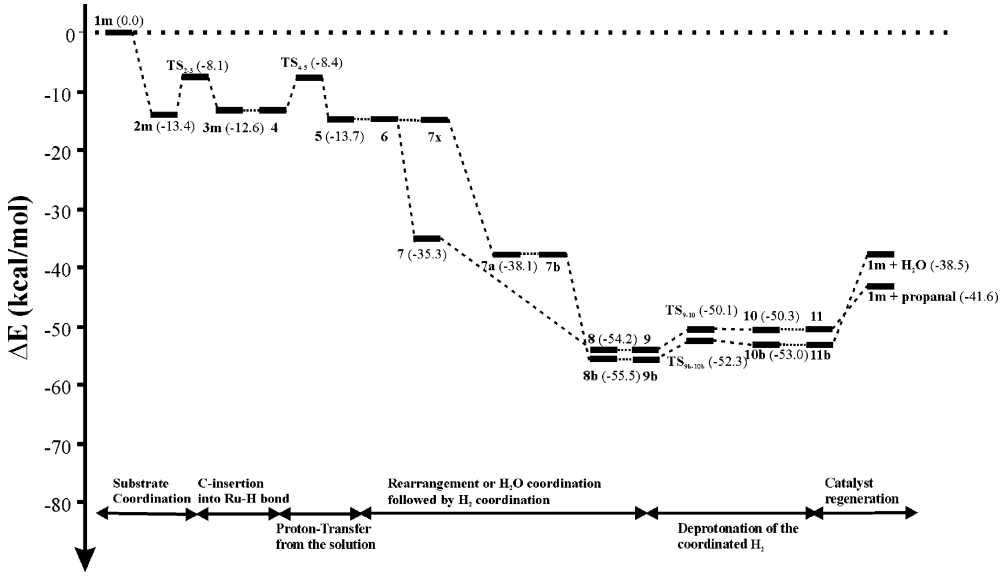

Figure 14. Potential energy change (kcal/mol) along the catalytic cycle during reaction path I.

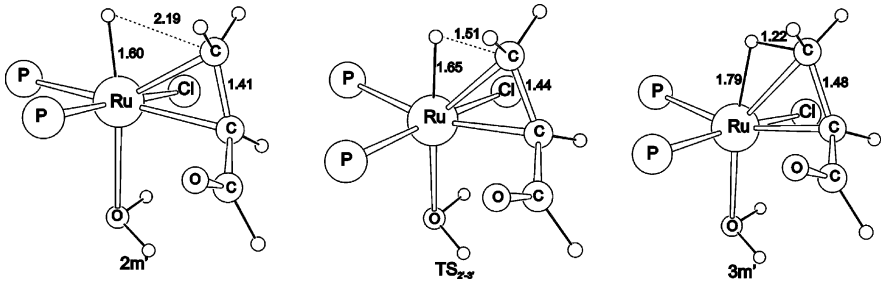

Figure 15. Optimized structures with selected bond lengths in structures representing the C insertion into the Ru−H bond starting from complex **2m′**.

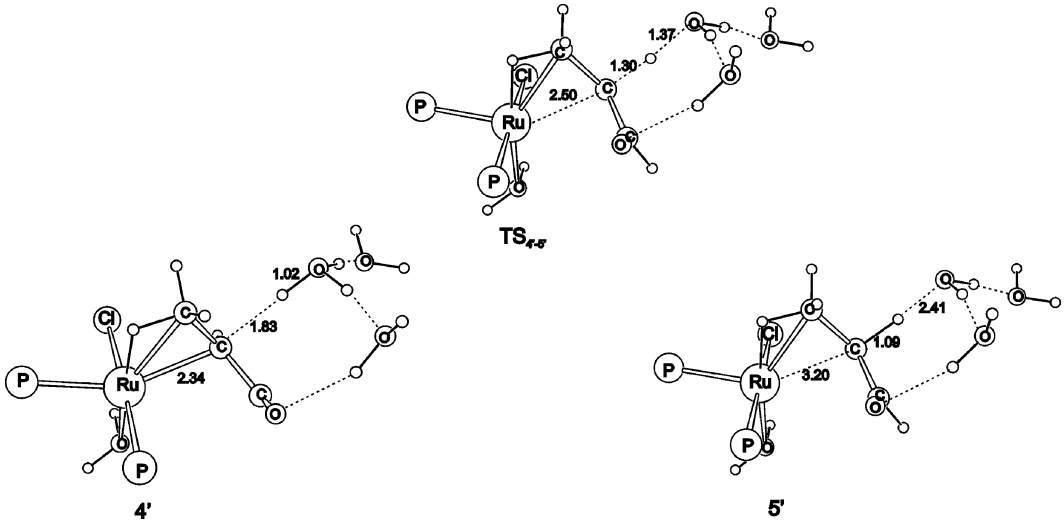

Figure 16. Optimized structures with selected bond lengths for structures representing the protonation of the carbon in complex **4′**.

of the agostic Ru−H−C bond and the formation of the complex **3m-H$_2$** with a coordinating H_2 ligand (Figure 7). The energy change for the formation of this η^2-H_2 intermediate is −5.4 kcal/mol. In this complex σ-bond metathesis can occur through **TS$_{mt}$** with a barrier of 7.5 kcal/mol, and this obviously leads to product dissociation (structure **P$_{mt}$**, which lies 18.5 kcal/mol below **3m-H$_2$**) and regeneration of the catalyst (Figure 7).

Concerning the barrier, this pathway is a possible mechanistic pathway for the C═C reduction that we cannot exclude. However, we feel that the reaction does not go through this pathway in acidic aqueous solutions. This mechanism, which involves (i) hydride transfer to the terminal carbon and then (ii) metathesis with a coordinated H_2 ligand, would not suggest the reaction to be pH-dependent. In contrast, the reduction of C═C does not take place in basic solutions using the same catalyst. In addition, the concentration of H_3O^+ in acidic aqueous solutions is generally well above that of H_2, which also favors protonation of the Ru−alkyl bond as the key step of the reaction. Hence, a detailed investigation of the reaction mechanism involving protic removal of the alkyl group is worthwile.

Since the Ru−C bond in **3m** is fairly strong (2.2 Å), having almost the same length as in the olefinic complex, a strong

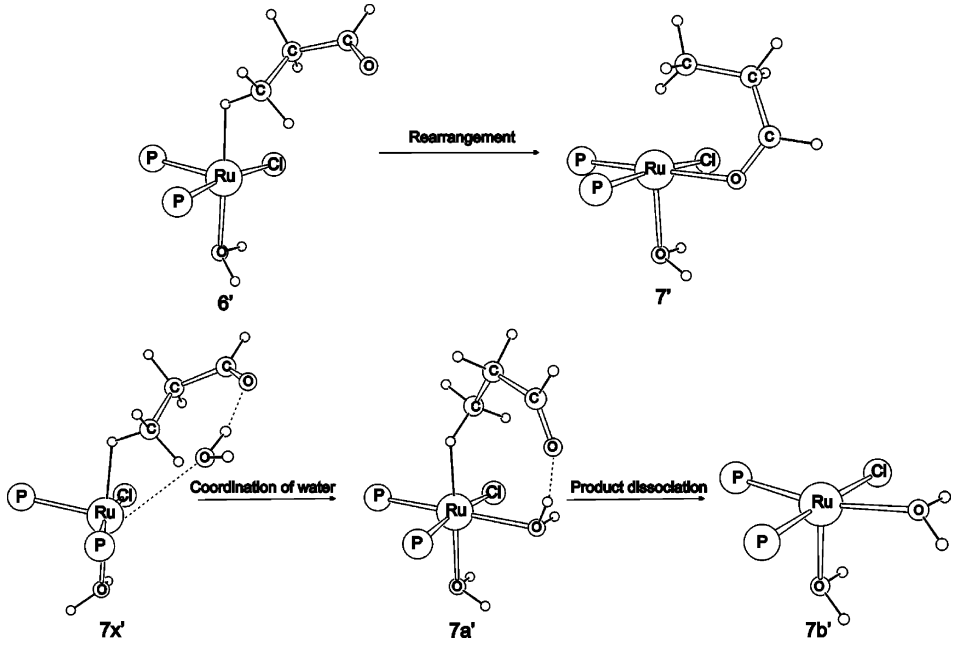

Figure 17. Optimized structures showing the possible further reactions of complex **6′**.

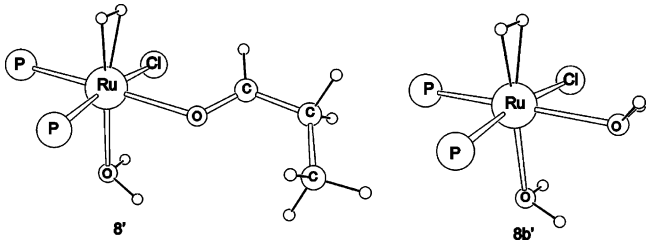

Figure 18. Optimized structures for complexes **8′** and **8b′**.

proton donor is required for the protonation of this carbon atom. The reaction takes place under aqueous acidic conditions; therefore, H_3O^+ is the best acid candidate. On the basis of previous computational projects, we know that the application of a single H_3O^+ ion as a protonating agent in the calculations is unrealistic, since H_3O^+ is itself an extremely strong acid and exists in aqueous solutions only as a part of a H-bonded network. The inclusion of the solvent is a difficult task, since modeling the environment is still an open question. For the particular case of introducing a proton as an active species within the reaction mechanism, small clusters of $[H_3O(H_2O)_2]^+$, found to be effective in earlier projects,[16,17] were applied.

The minimum corresponding to **3m** and its acidic environment, which facilitates the protonation of the carbon atom, was modeled by complex **4** (Figure 8), in which H_3O^+ points toward the unsaturated carbon atom of the agostic complex. The transition state $\mathbf{TS_{4-5}}$ was located as a stationary point on the potential energy surface, and the estimated energy barrier from **4** is about 4.2 kcal/mol. The structure and energy of **4** were estimated from the IRC calculations by starting from $\mathbf{TS_{4-5}}$, since the geometry optimization to the reactant side leads to a structure where the water chain moves close to the carbonyl group to form a strong hydrogen bond; nevertheless, during this IRC calculation there is a flat region that we are taking as structure **4**. This corresponds to a structure where the proton is close to the carbon atom of the acrolein. In the real solvent, there are enough water molecules around the complex to establish hydrogen bonds with the carbonyl group, and therefore a configuration with the proton close to the carbon atom of the substrate is feasible, as is in fact reflected by the IRC calculations.

The proton transfer leads to complex **5** (Figure 8), the structure of which was also estimated from the flat part of the potential energy surface. The process leads to the cleavage of the bond between ruthenium and the protonated carbon. This intermediate **6** (Figure 9) contains a vacant site and the final product of the reaction, which is coordinated by an agostic interaction.

There are three possible relevant ways for this complex to be stabilized. The first is a rearrangement to the coordination of the product aldehyde through its carbonyl oxygen. The structure of the complex (**7**) formed in this reaction is shown in Figure 9. The energy change for this rearrangement is −21.6 kcal/mol.

The second possibility is the coordination of a water molecule (since it is present in high concentration in the solution) to the Ru center, to form complex **7a**. The carbonyl oxygen forms a strong hydrogen bond with the coordinating water molecule; therefore, to calculate the energy balance for the reaction, it is much more realistic to calculate the energy difference between structure **7x** and **7a** (Figure 9). Structure **7x** represents the hypothetical structure of a complex optimized with a noncoordinating water molecule, which forms the same H bond with the carbonyl oxygen. This water coordination is favorable by 24.4 kcal/mol. The product is very weakly coordinated in **7a** (Ru−H distance 2.05 Å); thus, our calculations showed that decoordination of the product to form **7b** does not modify the reaction energy. The third possibility is the coordination of a H_2 molecule, which leads to the formation of complex **7h**. This last process is the least favorable of the above processes, having an energy change of −7.4 kcal/mol; in addition, the concentration of hydrogen molecules is much lower than that of water molecules.

The most probable path for the catalyst regeneration is the coordination and subsequent deprotonation of a hydrogen molecule. Either **7** or **7b** can coordinate a hydrogen molecule to form complex **8** or the analogous **8b** (Figure 10), having either H_2O or the product in the coordination sphere of the catalyst. The energy changes for the coordination reaction are −18.9 and −17.4 kcal/mol, respectively.

In aqueous solutions, and especially in acidic medium, water is the most obvious reactant to deprotonate the coordinated H_2

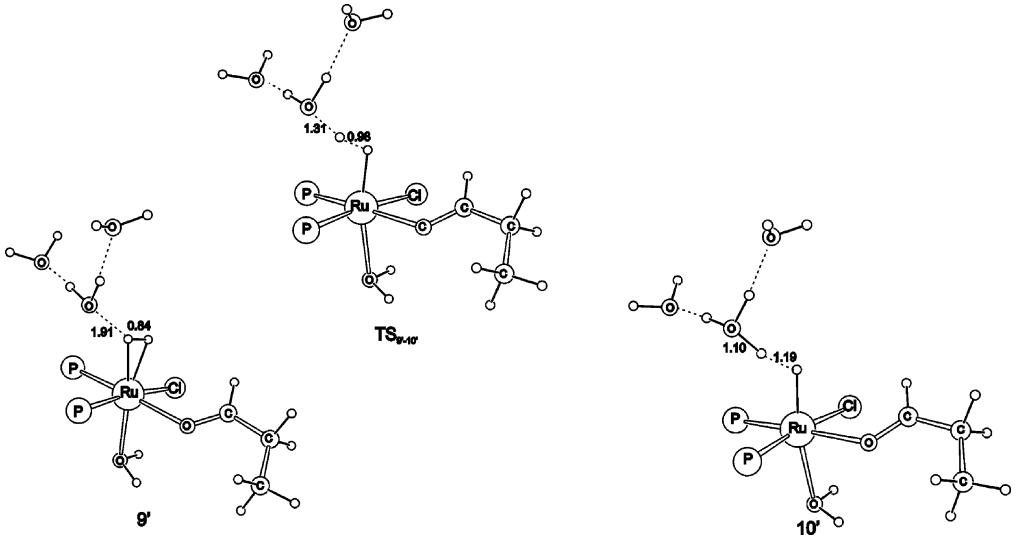

Figure 19. Optimized structures and selected bond lengths representing the deprotonation of complex **9′**.

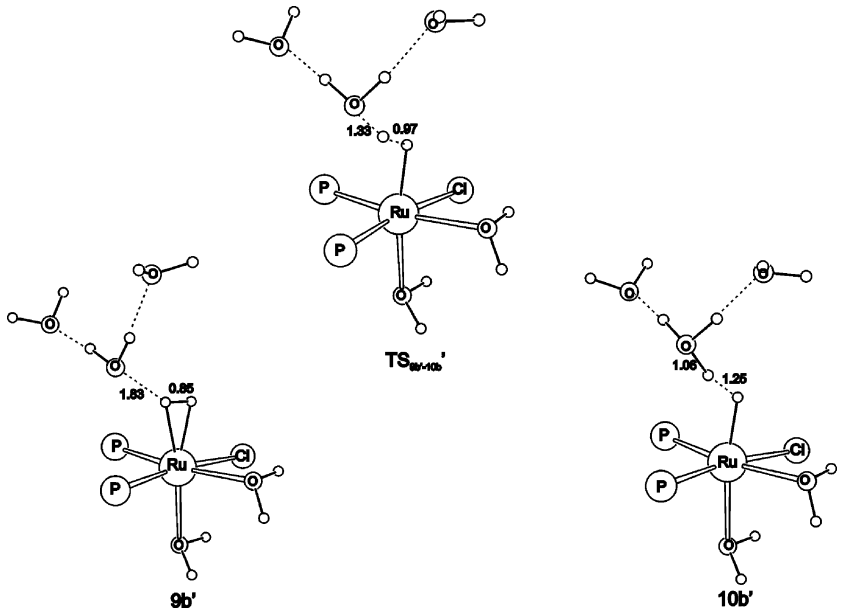

Figure 20. Optimized structures and selected bond lengths representing the deprotonation of complex **9b′**.

molecule. To study this process, the small cluster of three water molecules was applied again to describe the proton exchange between the positively charged dihydrogen complex and the surrounding water molecules. The relevant stationary points were found in the potential energy surface and are depicted in Figures 11 and 12. Adding three water molecules to **8** gives the minimum **9**, while adding them to **8b** leads to the corresponding minimum **9b**. The proton transfer in complex **9** goes through $\mathbf{TS_{9-10}}$ with a barrier of 4.1 kcal/mol to reach the product complex **10**; the energy change for the deprotonation reaction is 3.9 kcal/mol. This reaction is similarly described in the case of complex **9b**, through the transition state complex $\mathbf{TS_{9b-10b}}$ with a barrier of 3.2 kcal/mol, which leads to the product complex **10b**. The energy balance for the deprotonation is +2.5 kcal/mol.

The appropriate final complexes without the inclusion of the protonated water chains (**11** and **11b**) were optimized and are shown in Figure 13. The decoordination of the aldehyde from **11** or the dissociation of water from **11b** leads to the initial complex **1**, since this is the only stable isomer with the model PH_3 ligands. The dissociation energies are 8.7 and 14.9 kcal/mol, respectively.

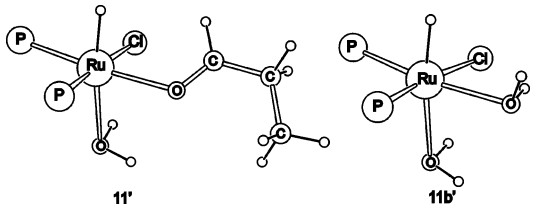

Figure 21. Optimized structures for complexes **11′** and **11b′**.

If we look at the possible mechanism of the reaction, the product formation in this pathway did not require steps of high barrier. The barriers in the case of the model system are 5.3 kcal/mol for the hydride migration to the terminal carbon, ca. 5.0 kcal/mol for the protonation of the other carbon atom of the agostic intermediate, and 4.1 or 3.1 kcal/mol for the deprotonation of the intermediates containing the coordinated H_2 molecule.

The overall profile for the reaction mechanism is shown in Figure 14.

Reaction Mechanism Starting from Complex 1m′ (Phosphine Decoordination: Path II). The coordination of a water molecule to the [RuHCl(*m*tppms)$_3$] complex and then the

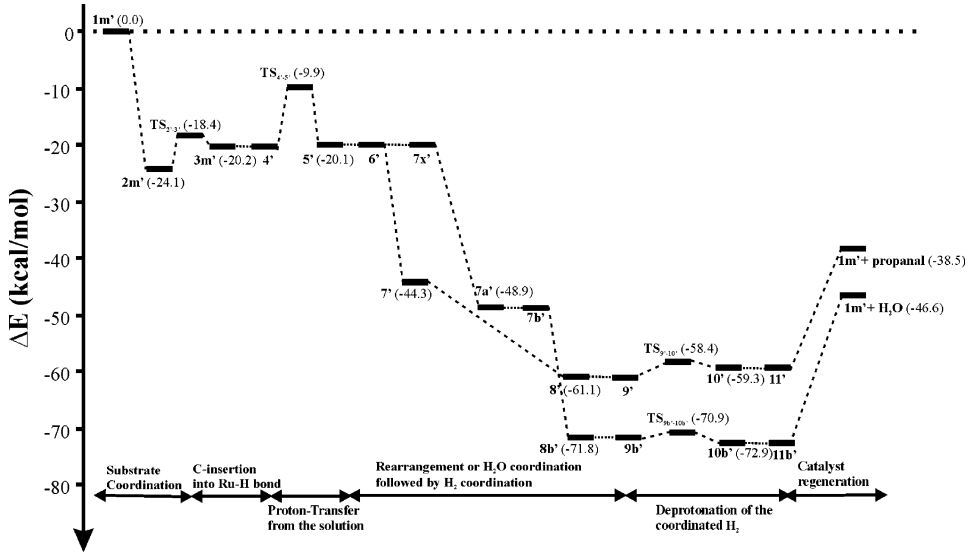

Figure 22. Potential energy change (kcal/mol) along the catalytic cycle during reaction path II.

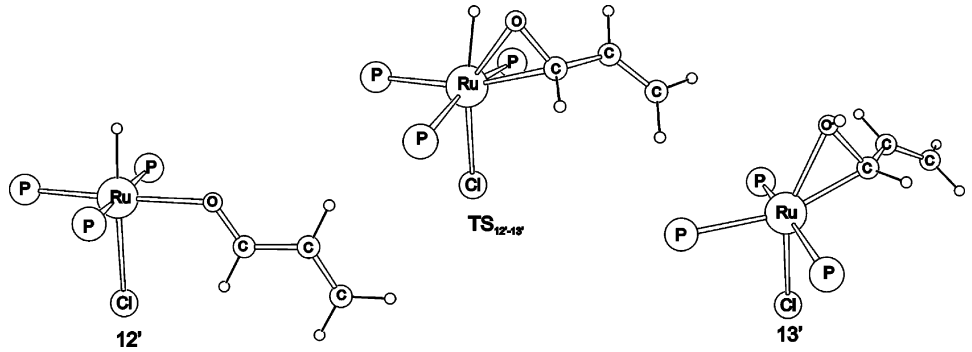

Figure 23. Optimized structures with selected bond lengths in structures representing the insertion of the oxygen atom of the coordinated C═O group into the Ru−H bond in complex **12′**.

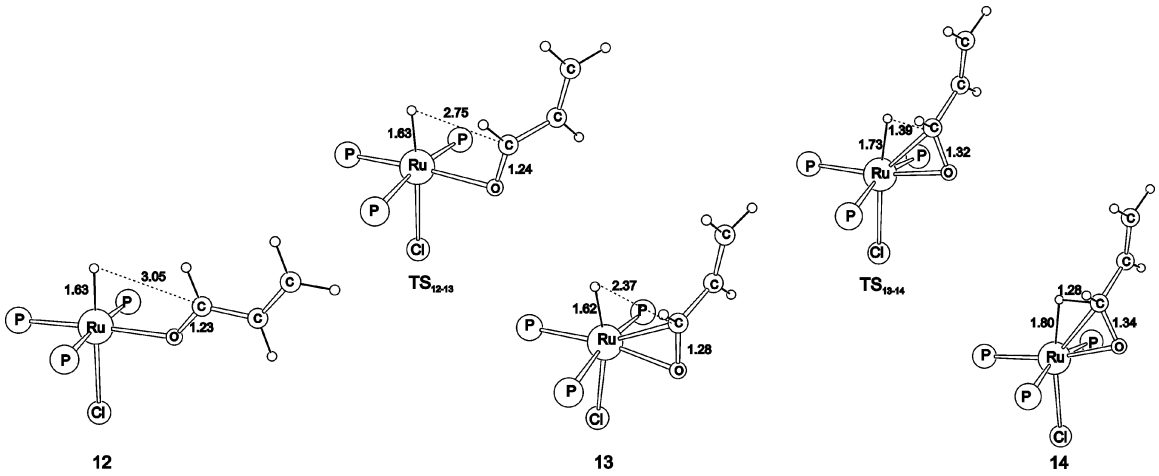

Figure 24. Optimized structures with selected bond lengths in structures representing the insertion of the carbon atom of the coordinated C═O group into the Ru−H bond in complex **12**.

dissociation of a phosphine molecule were found to be thermodynamically favorable, and **1e** is much less sterically hindered for the coordination of an olefin than **1b**, as shown by comparing the coordination energies: the energy for the **1b** + olefin → **2** process is +2.0 kcal/mol, whereas that associated with the **1e** + olefin → **2′** process is −5.8 kcal/mol.

The coordination of acrolein through its C═C bond to **1m′** leads to **2m′**. The coordination energy is −24.1 kcal/mol. In complex **2m′** the hydride ligand is in a favorable position to undertake the carbon insertion from the adjacent carbon of the coordinated olefin. This reaction goes through $\mathbf{TS_{2'-3'}}$, which lies only 5.7 kcal/mol above the reactant. The final product is in this case an agostic intermediate as well, shown as structure **3m′** (Figure 15). The energy change in this reaction step is 3.9 kcal/mol.

In this case, the proposed pathway to add the second hydrogen to the C═C bond is also the transfer of a proton from the hydroxonium ions present in acidic solutions. The same $[H_3O\text{-}(H_2O)_2]^+$ cluster as before was used as a model protonating agent. The behavior of the potential energy surface was found

to be analogous to that for structures **4** and **5**, and only $\mathbf{TS_{4'-5'}}$ was characterized as a real stationary point. The structures representing the proton transfer are **4′**, $\mathbf{TS_{4'-5'}}$, and **5′** (Figure 16). The estimated barrier is 10.3 kcal/mol, and the estimated reaction energy is 0.1 kcal/mol.

The product of the protonation reaction was optimized without the water cluster (**6′**). Processes analogous to those found relevant in the case of complex **6**, that is, the coordination of a water molecule to the empty site and the rearrangement of the coordinated product, were considered. The structures representing these processes are shown in Figure 17. Energetics were found to be similar to those in the case of the analogous complex **6**. The energy change for the rearrangement is −24.2 kcal/mol, and that for the H_2O coordination is −28.8 kcal/mol.

In this reaction path, the coordination and immediate deprotonation of H_2 to give either complex **7′** or **7b′** was considered as the most obvious way to regenerate the catalytically active hydride species. The complexes formed after H_2 coordination (**8′** and **8b′**) are shown in Figure 18, and the corresponding coordination energies are −16.8 and −22.9 kcal/mol.

The deprotonation of the coordinated hydrogen molecule is thought to occur by the surrounding water molecules, which are present in high concentration. The same cluster of three water molecules was applied as for the deprotonation of complexes **8** and **8b** (see path I). The structures for the deprotonation are shown in Figures 19 and 20, and the barriers are 2.7 kcal/mol in the case of **9′** and 0.9 kcal/mol in the case of **9b′**. The energy changes for the deprotonation are 1.8 and −1.1 kcal/mol, respectively.

The deprotonated complexes were optimized in the absence of the water clusters, and the corresponding structures (**11′** and **11b′**) are shown in Figure 21. The decoordination of either the product or the H_2O ligand (in a position cis to the hydride) leads to the catalytically active complex **1m′**. The dissociation energies are 20.8 and 26.3 kcal/mol, respectively.

The reaction profile corresponding to path II is shown in Figure 22.

On the basis of the comparison of Figures 14 and 22, we can state that the profiles for the mechanisms starting from $[RuHCl(PH_3)_3]$ and $[RuHCl(H_2O)(PH_3)_2]$ are very similar. Only slight differences can be found in the reaction barriers; thus, both mechanisms can possibly occur in the solution.

Selectivity of C═C versus C═O in Acidic Solutions. The aim of this theoretical work was not only to provide a mechanistic description for the C═C reduction catalyzed by $[RuHCl(mtppms)_3]$ in acidic solution s but also to account for the selectivity for C═C bonds against C═O bonds in the reduction of cinnamaldehyde. The comparison was made again by utilizing a model system, PH_3 ligands, and acrolein as substrate.

Obviously, the first step of the C═O reduction must be the coordination of the C═O group. The most stable isomers of complexes with coordinated acrolein having its C═O bond in a position cis to the hydride ligand, **12** and **12′**, are shown in Figures 23 and 24. The O-coordinated intermediates (**12** and **12′**) lie 5.6 and 3.3 kcal/mol, respectively, above the π(C═C) complex (**2m**) formed by the coordination through the olefinic bond. Since a rapid preequilibrium is thought to occur between the π(C═C) complex and the O-coordinated intermediates, all the overall barriers for the hydride transfer are referenced to the energy of complex **2m**. In **12′**, which is the most stable isomer, the hydride is positionally close to the oxygen of the C═O group, allowing the insertion of the oxygen into the Ru−H bond. The reaction goes through $\mathbf{TS_{12'-13'}}$, which lies 45.1 kcal/mol above the corresponding minimum **12′**. This high energy is not surprising if we consider that this interaction is between an electron-rich carbonyl oxygen and a negatively charged hydride ligand.

Table 2. Energy Barriers (kcal/mol) Calculated for the Hydride Transfer in $[RuHCl(C═C)(PH_3)_3]$ and $[RuHCl(C═O)(PH_3)_3]$ Complexes

	transfer to C═C	transfer to C atom of C═O	transfer to O atom of C═O
$\Delta E^{\ddagger}$ (kcal/mol)	5.3	17.3	48.4

In complex **12** the carbon atom of the C═O lies in a favorable position to be inserted into the Ru−H bond. This insertion occurs in two steps. Complex **12**, in which the C═O group presents a η^1 coordination mode through the oxygen atom, rearranges to complex **13**, in which the substrate coordinates through its π(C═O) bond. Complex **13** lies 4.2 kcal/mol above **12**, and this rearrangement goes through $\mathbf{TS_{12-13}}$. The next step is the transfer of the hydride to the carbon atom of complex **13** to form product **14**. The hydride transfer proceeds via the transition state $\mathbf{TS_{13-14}}$, which lies 7.5 kcal/mol above complex **13**.

The energy barriers for the hydride migration to the coordinated C═C and C═O bonds give convincing answers to the question of why selectivity for the reduction of the C═C bond was found in acidic solutions.

We can see in Table 2 that transfer of the hydride to the carbon atom of the coordinated C═C bond has a barrier of 5.3 kcal/mol. Nevertheless, for the most stable isomer, in which the C═O is coordinated, the oxygen can be inserted into the Ru−H bond with a barrier of 48.4 kcal/mol, while in the case of the isomer in which the carbon can be inserted into the metal−hydride bond, the barriers are 12.5 kcal/mol to rearrange to π(C═O) coordination and 7.5 kcal/mol for the C insertion. The total barrier from **2m** is 17.3 kcal/mol, which is much higher than the 5.3 kcal/mol barrier for the hydride transfer to the C═C bond.

Concluding Remarks

In the above theoretical study, a plausible reaction mechanism for the selective C═C reduction of cinnamaldehyde catalyzed by $[\{RuCl_2(mtppms)_2\}_2]$ in aqueous solutions was proposed. The objective of our work was not only to describe the mechanism for C═C reduction but also to get convincing results accounting for the selectivity against C═O reduction, which was found experimentally in acidic aqueous solutions.

The reaction mechanism was constructed by the application of PH_3 ligands instead of the sulfonated aromatic phosphines and acrolein as a model for cinnamaldehyde. In the cases where the truncation of the real system seemed to cause significant errors in the energetics, calculations with the real ligands/substrates were made. The solvent effects of water molecules were also considered, when solvent molecules or ions participated in the reaction. We applied small water clusters, which had been systematically tested in earlier works.[16,17]

Two alternative mechanisms were considered, one starting from $[RuHCl(PR_3)_3]$ (path I) and the other starting from $[RuHCl(H_2O)(PR_3)_2]$ (path II). The energy profiles do not suggest a major difference in the catalytic activities of $[RuHCl(mtppms)_3]$ and $[RuH(H_2O)Cl(mtppms)_2]$; thus, reactions through both pathways are feasible. Both paths include the same types of elementary steps, and the general overall reaction mechanism is shown in Scheme 1. We can conclude that path I is favored on the basis of the fact that only $[RuHCl(mtppms)_3]$ was detected

Scheme 1. Reaction Mechanism of the C═C Reduction Catalyzed by [RuHCl(*m*tppms)$_3$] or [RuHCl(H$_2$O)(*m*tppms)$_2$] in Aqueous Solution

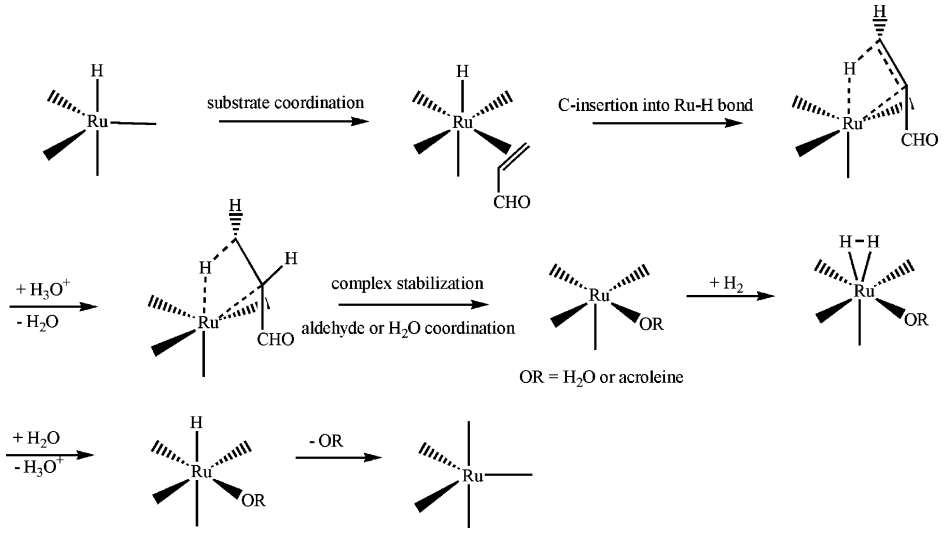

in the solution by NMR spectroscopic methods,[11] while path II is favored on the basis of steric considerations and the results of kinetic experiments, which showed that the ideal ratio of [Ru] to [P] in the solution is 1:2.[33]

It was also shown again that aqueous solutions present a rather unconventional reaction medium, since water molecules could take part in many reaction steps. Water molecules can act as coordinating ligands to alter the vacant sites for the reactants or intermediates. Another important feature of water molecules is that they can provide or accept hydrogen ions in proton-transfer reactions and facilitate reaction routes, which would be unfeasible in nonpolar organic solvents.

We have to note that the description provided here for the reactions in aqueous media could be improved by means of molecular dynamics simulations; however, this work is the first to theoretically describe in detail the aqueous-phase C═C reduction reaction catalyzed by transition-metal complexes, and we hope this theoretical paper can serve as a starting point for mechanistic investigations of this type.

Acknowledgment. This work was carried out under the HPC-EUROPA project (Grant No. RII3-CT-2003-506079), with the support of the European Community—Research Infrastructure Action under the FP6 "Structuring the European Research Area" Program. This work was also supported by the AQUACHEM project (MCRTN-CT-2003-506864). A.L. and G.U. acknowledge financial support from the Spanish MEC (Project No. CTQ2005-09000-CO2-01). A.L. thanks the *Generalitat de Catalunya* for a *Distinció per a la Promoció de la Recerca Universitària.* F.J. is grateful for financial support by the National Research Fund of Hungary (Grant No. OTKA T043365).

Supporting Information Available: Tables giving Cartesian coordinates and total energies of the optimized structures shown in the paper. This material is available free of charge via the Internet at http://pubs.acs.org.

OM050929Y